Physical Sciences Section

Pakistan J. Sci. Ind. Res., Vol. 23, No. 5 October 1980

FLOW LIGHT SCATTERING

Part I. Theoretical Principles of the Effect and Apparatus for its Measurement

Noor Ahmad and Sajida Noor

Institute of Physical Chemistry, University of Peshawar, Peshawar

(Received April 17, 1979)

A brief introduction is given into the theory of radiation scattering by rigid spheroids dispersed or dissolved in a liquid medium subjected to flow at well-defined velocity gradient. The theory is limited to spheroids whose largest dimension does not exceed 1/3 of the wavelength of the incident radiation. It is shown that the radiation scattering increment produced by flow makes it possible to determine not only the axial ratio as obtainable by streaming birefringence, but also the numerical values of semimajor and semiminor axis of a spheroid provided two orthogonal components of incident linearly polarized light are used. Essentials of the construction and operation of an apparatus designed for the study of hydrodynamic radiation scattering are described.

INTRODUCTION

Light scattering measurements in systems with randomly oriented scattering bodies are widely used for determining their molecular weights or sizes. Much of the progress made during the last 20 years in the field of macromolecular physics and chemistry is due directly to the application of this powerful technique. As shown primarily by Zimm [1] light scatteting measurements may also be used successfully for determining the shape of light scattering bodies provided that they are large enough so that the radiation diagram is dissymmetrical (more scattering in the forward direction than in the backward direction) and that the refractive index of scatterer and medium are sufficiently close to each other (applicability of the Rayleigh–Gans theory [2] or the equivalent Debye theory). The respective method is relatively insensitive to particle shape, however, since the effect observed at a given angle of observation, in a system at rest, is the average of all possible orientations of the nonspherical bodies with respect to the incident beam and the direction of observation. By this averaging, characteristic effects of nonspherical shape upon light scattering are lost. Therefore, light scattering studies on systems with oriented nonspherical scattering bodies are preferable whenever a reasonable degree of orientation is experimentally attainable without extraordinary difficulties. The present paper is concerned with this alternate method, the principles of which had been outlined briefly a few years ago [3]. The nonspherical light scattering bodies to be considered are intrinsically isotropic spheroids.

SELECTED ASPECTS OF THE THEORY

General Definitions. Figure 1 defines those of the symbols used in the following which pertain to the experimental variable involved in hydrodynamic orientation of spheroids. R represents the incident beam; O is the location of the solution or of the dispersed system containing the light scattering bodies; V and G are the directions of flow and of the velocity gradient, respectively, $\gamma = (180^{\circ}-\theta)$, where θ is the angle of observation with respect to R; ω is the angle of observation with respect to the direction of flow, V. For $\theta = 90^{\circ}$, the situation shown in Fig. 1 ω is in the V–G plane. It is 90° in the drawing. For $\theta \neq 90^{\circ}$, ω would be the angle of observation with respect to V projected into the V–G plane; ψ is the angle between the symmetry axis of a single spheroid and the inverse of R and ϕ is the angle between the projection of the symmetry axis of a spheroid, upon the V–G plane and the direction of G. The axis of the concentric cylinder apparatus is parallel to R and O defines a small illuminated section of the light scattering fluid contained in the gap between two concentric cylinders.

The Distribution Function. Under the influence of flow, rigid particles rotate and nonrigid ones are deformed. In either case there results a preferential orientation or quasiorientation respectively of the nonspherical body. This is the result of the fact that on assuming laminar flow

$$V = \begin{bmatrix} O \\ G_X \\ O \end{bmatrix} = \begin{bmatrix} -\frac{1}{2}G_Y \\ -\frac{1}{2}G_X \\ O \end{bmatrix} + \begin{bmatrix} \frac{1}{2}G_Y \\ \frac{1}{2}G_X \\ O \end{bmatrix} \qquad (1)$$

of constant velocity gradient G in the X direction and proceeding with a velocity V in the Y direction. The first vector in eq.. (1) shows the rotation of the fluid around a given point, due to which the particles in it are rotating. The velocity of rotation of the symmetry axis of a spheroid is not constant, however, because of the influence of the second vector, which leads to hydrodynamic pull at $\phi = +45^{\circ}$ and -135°, and to hydrodynamic push at $\phi = -45^{\circ}$ and $+135^{\circ}$. For rigid spheroids, the velocity of rotation is slower at $\phi = 45^{\circ}$ and faster at $\phi = -45^{\circ}$. The resulting tendency of orientation is counteracted by the rotatory Brownian motion. Therefore, the spatial distribution of the symmetry axis of these bodies is defined by the paramteter

$$\beta = G/D_r, \tag{2}$$

where D_r is the rotatory diffusion coefficient. According to Gans [4] for prolate spheroids ($p>1$) where p is axial ratio

$$D_r = (3KT/16\pi\eta_1 a^3)\,(p^4/(p^4-1)$$
$$\times \left\{[(2p^2-1)/p(p^2-1)^{1/2} \ \ln\left[(p+(p^2-1)^{1/2}\right] -1)\right\} \tag{3}$$

and for oblate spheroids ($p<1$)

$$D_r = [(3KT/16\pi\eta_1 a^3)(p^4/(1-p^4)]$$
$$\times \ [(1-2p^2)/p(1-p^2)^{1/2}\ (\text{arccos}p)+1) \tag{4}$$

In the case of a sphere ($p=1$), both of these equation coincide with the well-known Einstein equation

$$D_r = KT/8\pi\eta_1 a^3 \tag{5}$$

Here, K is Boltzmann's constant, T is the absolute temperature, and η_1 is the viscosity of the medium. The semiaxis of symmetry a may be expressed in terms of α if the wavelength is kept constant which is assumed in the present paper. In that case, therefore, D_r is a function of α and p.

Light Scattering in Flowing Systems. The intensity of light scattered by nonspherical particles in flow is the properly weighted average of the intensity scattered over all possible orientations. It can be calculated by multiplying the scattering function by the distribution function and by integrating the product over the angles ψ and ϕ:

$$<\iota> = \int_0^{2\pi} d\phi \int_0^{\pi} \text{Sin}\,\psi\, d\psi\, \iota F \tag{6}$$

Of particular interest is the dependence of the scattering function on the angle of observation ω. The value of ω at which $(<i(\xi,\eta)>$ reaches a maximum, ω_{max}, at constant θ, is a function of m, p, β and θ. Moreover, it depends on whether the incident beam is polarized or unpolarized. If it is polarized, it also depends on the direction of the electric vector (ξ,η). The simplest situation exists if one operates with incident unpolarized light and observes the total scattered light $[(\xi,\eta) \rightarrow (u,t)]$ at an angle θ–90° and if, in addition, the particles are sufficiently small. Then the angle of maximum scattering ω_{max} becomes, at small β, a function of β only, viz.

$$\text{Cot}\ 2\omega_{max}\,(u,t) = \beta/6 \tag{7}$$

limiting equation for the scattering maximum is therefore identical with that for the extinction angle in streaming birefringence [5]

$$\text{Cot}\ 2\chi = \beta/6 \tag{8}$$

It should be noted that eq. (8) and, therefore, eq. (7) apply also at any β if the axial ratio $p \rightarrow 1.0^6$.

While eqs. (7) and (8) are equal in form, it should be noted that $\chi = (\omega_{max} - 90^{\circ})$. In addition the extinction angle χ represents the angular position of an intensity minimum (in transmitted light), while ω_{max} defines the angular position of an intensity maximum (in laterally scattered light) which is experimentally easier to define. Considering as a practical example a prolate spheroid, one will find that χ defines the most probable direction of its symmetry axis while ω_{max} defines the direction perpendicular to it. Consequently, χ decreases from a value of 45° as $\beta \rightarrow 0$ to 0° as $\beta \rightarrow \infty$ while ω_{max} at the same time decreases from 135 to 90°.

After having obtained, at sufficiently low G, β and, therefore, D_r from experiment, by means of eq. (7) one can calculate p, a and b (in view of eqs (2–4), provided that one more quantity, for example the particle weight M, expressed by eq.9

$$M = \tfrac{3}{4}\pi\,(N_A/V)a^3/p^2), \tag{9}$$

is known. Here V is the partial specific volume (or the inverse of the density) of the scattering material. On substituting eq. (9) into (3) or (4) one obtains

$$\frac{4\,VMD_r\eta_1}{N_A KT} = \frac{p^2}{p^4-1}\ \frac{2p^2-1}{p(p^2-1)^{1/2}}\ \ln\left[p+(p^2-1)^{1/2}\right]-1\ ,\ p>1, \tag{10}$$

$$= \frac{p^2}{1-p^4}\ \frac{1-2p^2}{p(1-2p^2)^{1/2}}\ (\text{arc Cos}\ p)+1\ ,\ p<1, \tag{11}$$

Where K is Boltzmann's constant and N_A is Avogadro's No. Consequently, the value of p follows immediately. An alternate possible method used for determining p and a of spheroids consists of measuring the scattered light intensity itself as a function of β. Both theoretically and experimentally simplest is the measurement of the total scattered light with the incident beam being unpolarized, particularly if $\theta=\omega=90^0$ The RGS approximation gives then the following equation for the fractional change of the scattered light intensity in the flowing system relative to that at rest, if $\beta<1$:

$$\left(\frac{\Delta i}{i_o}\right)_{u,t} = K\beta^2 \qquad (12)$$

THE APPARATUS

General Survey. The apparatus contains the following basic components: (a) the concentric cylinder assembly, (b) the driving mechanism for the concentric cylinder assembly, and (c) the optical and recording system.

The concentric cylinder assembly consists of two coaxial cylinders, of which only the inner rotates, and accessories. The scattering system to be studied is introduced into the annulus between these cylinders. A lateral window built into the stationary (outer) cylinder allows the measurement of the change in the intensity of the scattered light produced by the orientation (or deformation) of the dissolved or dispersed scattering bodies.

The driving mechanism consists of an AC motor whose speed is carefully regulated before suitable gear reductions are introduced. The transmission unit is a special belt connecting the driving and rotor pulleys.

The optical system was selected with the special requirements in mind for this type of measurement, making use of the high intrinsic brightness of a high pressure mercury lamp.

The Concentric Cylinder Assembly. The concentric cylinder unit is held by means of a special sleevelike holder The latter makes a vertical displacement of the unit possible. The holder, in turn, is bolted to a universal compound vise which allows adjustment of the cylinder unit in the horizontal plane. Construction details of one of the two concentric cylinder unit used follow from Fig. 3. The radii of the six peripheral rotor sections available for both cylinder units were varied in steps of 0.1 mm so that by a simple exchange of the section by means of a pulling device six gapwidths, viz., 0.2 (0.1) 0.6 mm could be selected. A removable bottom plate (Fig. 3) fastened to the stationary cylinder with set screws allows for this interchangeability of the peripheral rotor section and for cleaning the cell.

The incident beam enters through opening 1 (Fig. 2), passes the annulus, and leaves through another opening 2 in the bottom plate. These tapered openings, 0.5 cm dia, are fitted with optical glass windows held in place by rubber O rings and screws.

The stationary outer cylinder (stator) is jacketed for circulating water. It has a lateral opening 3 for the measurement of the scattered intensity of the solute. The

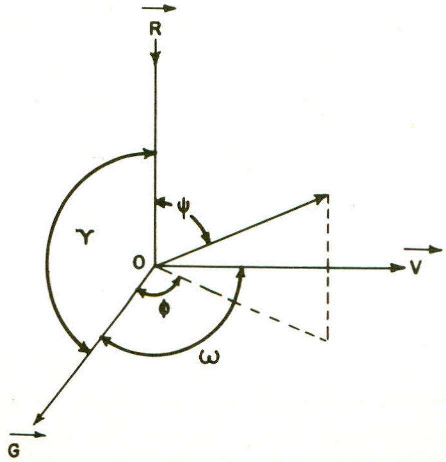

Fig. 1. Geometry of the flow arrangement considered.

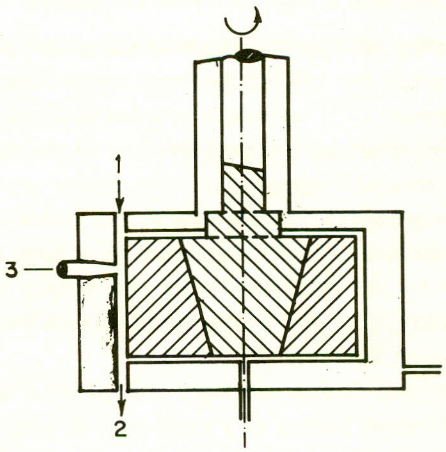

Fig. 2. The concentric cylinder assembly.

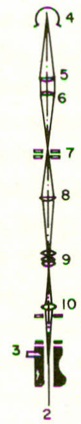

Fig. 3. The optical system.

conical design of this opening allows for a variation of both angles of observation ω and θ (Fig. 1). The former can be varied within the limits of $+30^{o}$ (in air) with respect to the direction of the velocity gradient. The opening 3 terminates in a tapered window of optical glass held in place by an O ring and screw.

The determination of the velocity gradient in the gap,

$$G = (\pi R_2/30d)\ \Omega \sec^{-1} \tag{13}$$

requires that the radius of the rotating inner cylinder R_2, the gapwidth d, and the angular velocity of the rotor Ω (60 rev/min) be accurately known. The diameter of each inner cylinder was measured with a micrometer caliper and the width of each gap was determined with a prism and microscope focussed at the exit end of the annulus.

The Driving Mechanism. An electronic system provides a constant speed for 1/3 h.p. gearhead motor. This motor with a maximum 1725 rev/min is coupled with gear reduction units, its minimum constant speed is 50 rev/min. The feedback mechanism attached to the motor provides a speed regulation of 0.5% at all speeds. The motor and the two gear reduction units are supported by a large I beam which provides the necessary height and rigidity for this portion of the system; this I beam is welded to a heavy iron base standing on three levelling screws.

The crowned driving and rotor pulleys are connected by thin flat rubber belt of very small mass in order to eliminate as much as possbile the transmission of vibrations from the motor unit to the concentric cylinder unit. Thanks to this arrangement, the amplitude of the oscillations of the concentric cylinder assembly was less than 1 μ at any of the speeds used. This was verified by special experiments in which the annulus of the cylinder unit was viewed microscopically with the aid of a total reflection prism placed below the exit window 2 (Fig. 2).

To measure the rotor speed directly and reliably, a tachometer generator (model 508 A), was mounted on the axle of the rotor and connected to Howlett Packard electron counter (model 521 A). This tachometer – counter combination is accurate to within ± 1 rev/min at any speed. This defines the overall maximum uncertainty in G. It is 0.67% at 150 rev/min and rises to 6.7% at the very low speed of 15 rev/min.

The Optics. The optical equipment is mounted on a vertical optical bench which by means of a long handle bar can be rotated about a hollow steel cylinder. The latter terminates in a heavy base, which rests on massive set screw and on a vibration free floor.

The light source assembly (Fig. 3) contains a 100 WAH-6 mercury arc lamp (4) operated with the GE core and coil transformer (model 9T 64Y 4010) in conjunction with a Sorensen voltage stabilizer (model 2000 A) and is mounted on a massive steel cylinder which fits snuggly into and rotates about the hollow cylinder. Consequently the entire light source assembly can be rotated in a horizontal plane. This is made easy since two adjustable counter weights serve to put the center of gravity of the assembly into the center of cylinder. In addition, the radial distance of the light source from the center of rotation can be varied by means of the sliding mechanism.

Immediately following the light source is cooling unit consisting of two plane parallel plates between which water is circulated in order to cut out the heat developed by the mercury arc. This is followed by the collimating unit, which consists of two lenses 5 and 6 and three diaphragms. The twin precision slits 7 have a variable aperture, and their mutual distance is also variable. They thus allow one, on proper adjustment, and in conjunction with the lenses 9, 10 to obtain a practically parallel beam over the entire length of the liquid layer in the gap of concentric cylinder assembly. Provision is made, immediately following the twin slits, for the insertion of two filters of which one is an interference filter and the other an auxilliary filter used for optimum spectral purity of the beam which enters the gap. The cross-section of the beam in the gap is at the most, 1.2 mm^2 (0.6 mm gap) and, at the least 0.3 mm^2 (0.2 mm gap), the linear dimension in the direction of flow being 3 mm and that in the direction of the velocity gradient being not in excess of 1/2 – 2/3 of the gap width.

The detection units for the scattering measurements and reference intensity measurements, respectively are two highly sensitive photvolt photometer (model 520 sp) and two IR 21 Photomultiplier tubes.

The problems involved in measurements of streaming birefringence are encountered also in the present instrument. Additional problems characteristic for the present instrument and method are primarily the following: (1) Unless the beam is very carefully centered and free of a diffuse corona, diffuse reflection at the cylinder walls produces a flow independent response in the recording instrument of the same order of magnitude as the scattering in dilute systems. In order to reduce the minor reflection effect remaining after proper adjustment, the inner cylinder was blackened by suitable chemical treatment. The residual 'background' varies with the gapwidth and the liquid (its refractive index). For the 0.4-mm gap and pure water, the residual background intensity is 1×10^{-7} times the intensity of the incident beam for observation at ω=90^{o}. The correction factors to be applied, if absolute scattered intensities are to be determined, are evidently larger than in conventional light scattering measurements. In actual practice, however, the residual diffuse reflection is easily eliminated from the results by determining the fractional change in scattering produced by flow rather than scattering intensities. (2) Dust particles and colloidal air bubbles, which do not interfere with streaming birefringence, have a very disturbing effect here and must be eliminated. Their presence manifests itself readily by the occurrence of distinct jumps of the photoelectric current each time when such an extraneous scattering body flows across the illuminated section of the gap. The problems of air bubbles of very small size is encountered primarily on using systems of high viscosity. It can be circumvented easily on filling the light scattering system into the gap slowly by means of gravity.

BRIEF REVIEW OF RESULTS OBTAINED WITH THE APPARATUS

A few preliminary results obtained with the apparatus described above have been published. A comprehensive presentation of more recent systematic investigations will be given in a subsequent paper. It is useful, however, to present a few typical results which illustrate the magnitude of the effects that one can obtain. Fig. 4 represents results obtained with an aqueous colloidal dispersion of β–FeOOH crystals which had nearly uniform size and shape (average length 345 nm, model length 236 nm, mean axial ratio 4.0). The curves show the fractional increase in light scattering $\Delta I/IR$(IR representing the scattered intensity of the system at rest) as a function of the velocity gradient G. The results are seen to be reversible at all angles ω studied. As expected, the effect increases with increasing ω, the maximum effect being expected at that angle where the observation would be perpendicular to the largest dimension of the particles. Analysis of these data lead to a determination of particle length in agreement with the numerical electron microscopic values quoted above. Fig. 4 illustrates a pure orientation effect of rigid crystals. Use of polarized light enhances the analytical potential of the method.

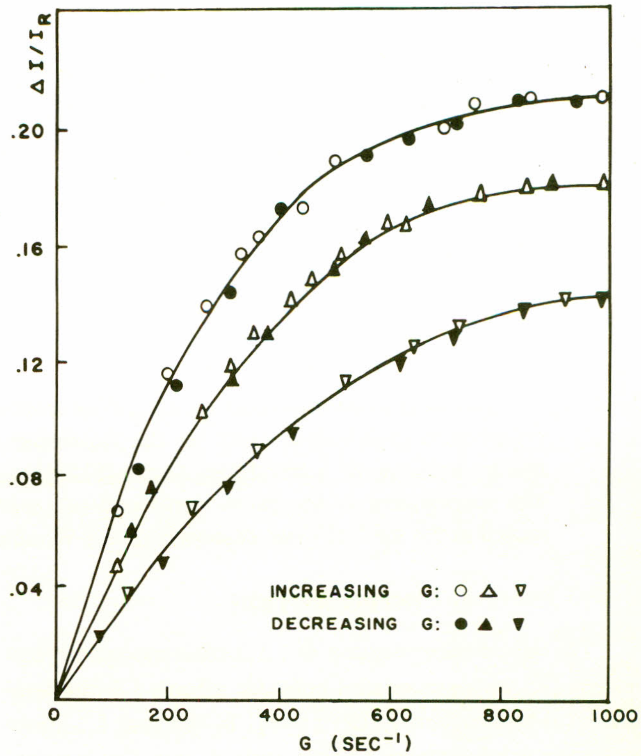

Fig. 4

Acknowledgement. The authors are grateful to Pakistan Science Foundation for the financial support for carrying out this project.

REFERENCES

1. B H. Zimm, J. Chem. Phys., **16,** 1093 (1948).
2. Lord Rayleigh, Proc. Roy. Soc. (London), **A84,** 15 (1911); **A90,** 219 (1914); R. Gans, Ann. Physik, **76,** 29 (1925).
3. W. Heller, Rev. Mod. Phys., **31,** 1072 (1959).
5. Equation (15c) ***in*** A. Peterlin and H.A. Stuart, Z. Phys **112,** 1 (1939).
4. R. Gans, Ann. Phys., **86,** 628 (1928).
6. See Eq. (18) ***in*** H.A. Scheraga, J.T. Edsall and J.O. Gadd, J. Chem. Phys., **19,** 1101 (1951).
7. Noor Ahmad, Pakistan J. Sci. Ind. Res., **17,** 97 (1974); **21,** 106 (1978).